# Anomalous Thermodiffusion of Electrons in Graphene

Deng Pan,[1,*] Hongxing Xu,[2] and F. Javier García de Abajo[1,3,†]

[1]ICFO-Institut de Ciencies Fotoniques, The Barcelona Institute of Science and Technology, 08860 Castelldefels (Barcelona), Spain
[2]School of Physics and Technology, Wuhan University, Wuhan 430072, China
[3]ICREA-Institució Catalana de Recerca i Estudis Avançats, Passeig Lluís Companys 23, 08010 Barcelona, Spain

(Received 13 June 2020; accepted 7 September 2020; published 22 October 2020)

We reveal a dramatic departure of electron thermodiffusion in solids relative to the commonly accepted picture of the ideal free-electron gas model. In particular, we show that the interaction with the lattice and impurities, combined with a strong material dependence of the electron dispersion relation, leads to counterintuitive diffusion behavior, which we identify by comparing a two-dimensional electron gas (2DEG) and single-layer graphene. When subject to a temperature gradient $\nabla T$, thermodiffusion of massless Dirac fermions in graphene exhibits an anomalous behavior with electrons moving along $\nabla T$ and accumulating in hot regions, in contrast to normal electron diffusion in a 2DEG with parabolic dispersion, where net motion against $\nabla T$ is observed, accompanied by electron depletion in hot regions. These findings bear fundamental importance for the understanding of the spatial electron dynamics in emerging materials, establishing close relations with other branches of physics dealing with electron systems under nonuniform temperature conditions.

DOI: 10.1103/PhysRevLett.125.176802

*Introduction.*—Thermodiffusion, also known as thermophoresis or Ludwig-Soret effect, and widely studied in molecular [1–3] and nanoparticle [4–6] systems, essentially denotes the fact that a temperature gradient $\nabla T$ can induce a nonuniform density distribution in an ensemble of particles. For a mixture of several types of particles, lighter and heavier species tend to move along and against $\nabla T$, leading to negative and positive thermodiffusion that produces accumulation in hot and cold regions, respectively [7–10]. For a one-component ensemble, as can be intuitively understood from the equipartition theorem $m\langle v^2\rangle/2 = \xi k_B T$ in $\xi$ dimensions, where $m$ and $v$ are the constituent mass and velocity, respectively, particles at higher temperatures move faster and thus should always diffuse against $\nabla T$ towards cold regions, causing depletion of the particle density in hot regions [3,6]. For conduction electrons in solids, a similar description is also routinely adopted to explain the Seebeck effect, in which a nonzero $\nabla T$ can give rise to a measurable voltage across a material. Although this intuitive prescription correctly predicts the sign of the thermoelectric voltage, it does not correctly describe the relation between the Seebeck effect and electron thermodiffusion. As we clarify in this work, electron thermodiffusion is not only driven by the electromotive field in the Seebeck effect, but also by an effective electric field associated with the temperature dependence of the chemical potential. More interestingly, aimed by this total thermoelectric field, electron diffusion could anomalously be directed along $\nabla T$, similar to the negative thermodiffusion of lighter particles in a mixture.

The diffusivity can be quantitatively characterized by a diffusion coefficient $\mathcal{D} = \langle v^2\rangle\langle\tau\rangle$, as known from Fick's laws. For free particles, the relaxation time $\tau$ results only from interparticle collisions. In contrast, electrons in solids are subject to various relaxation mechanisms, such as scattering by impurities or phonons [11]. More importantly, the group velocity of Bloch electrons can have significant departures from free electrons when the dispersion is far from parabolic. A notable example is provided by massless Dirac fermions (MDFs) in graphene [12,13], which feature a constant group velocity independent of the electron energy. Such a unique conical dispersion could endow graphene with unconventional thermoelectric properties, and indeed anomalous Seebeck coefficients in this material have already been observed [14–16]. Anticipating a dependence of diffusivity on electron velocity, we can also expect unconventional diffusion behavior of MDFs to emerge in graphene.

In this Letter, we focus on single-layer two-dimensional electron gas (2DEG) and graphene systems for a comparative study of the thermodiffusion behavior associated with either free electrons or MDFs. We find that the free-electron thermodiffusion in 2DEGs behaves indeed in accordance with conventional intuition, whereby electrons at higher temperatures tend to spread to low temperature regions, regardless of the scattering mechanisms. In contrast, MDFs in graphene exhibit an unexpected anomalous thermodiffusion effect. Although a higher temperature in graphene also signifies more energetic electrons, the diffusivity of these electrons is weaker, so they diffuse to and accumulate in the hot regions.

 

*Qualitative explanation of anomalous thermodiffusion.*—We consider thermodiffusion of electrons in a 2DEG or single-layer graphene subject to a temperature gradient $\nabla T$. As illustrated in Fig. 1(a), a strong $\nabla T$ can be easily achieved by using a tightly focused visible continuous-wave laser. The 2DEG can be experimentally realized by a thin doped semiconductor, so in both 2DEG and graphene materials the incident laser can cause strong interband transitions and heat the electrons up to $\sim 10^3$ K [17–21]. With $\nabla T$ established, electron thermodiffusion occurs because the diffusivity characterized by the coefficient $\mathcal{D} = \langle v^2 \rangle \langle \tau \rangle$ varies with spatial location. For a 2DEG with parabolic dispersion $E_k = \hbar^2 k^2 / 2m_e$ [black curve in Fig. 1(b), assuming a bare electron mass $m_e$ throughout the Letter], the group velocity $\sqrt{2E_k/m_e}$ is proportional to the wave vector $k$, so hot regions containing more energetic electrons should display stronger diffusivity (i.e., $\mathcal{D}^{\text{hot}} > \mathcal{D}^{\text{cold}}$) if we assume a constant relaxation time $\tau$. In fact, even when taking into account the energy dependence of the relaxation time $\tau(E)$, higher temperature still yields larger $\mathcal{D}$ in the 2DEG (see below). In consequence, the thermodiffusion direction of free electrons is consistent with particles in the ideal gas model.

In stark contrast to the 2DEG, MDFs in graphene exhibit anomalous thermodiffusion with net motion along the temperature gradient as a result of the constancy of the group velocity $v_F \approx 10^8$ cm/s [Fig. 1(c)]. Assuming a constant $\tau$, the diffusivity coefficient $\mathcal{D}$ is independent of temperature, therefore producing no thermodiffusion of MDFs. In practice, we need to consider an energy dependence of $\tau(E)$ resulting from various scattering mechanisms, so in general, electrons with higher energy possess shorter relaxation time, as shown below based on impurity and phonon scattering calculations. MDFs therefore display weaker diffusivity in hot regions (i.e., $\mathcal{D}^{\text{hot}} < \mathcal{D}^{\text{cold}}$), leading to anomalous diffusion, with electrons accumulated in the hot areas.

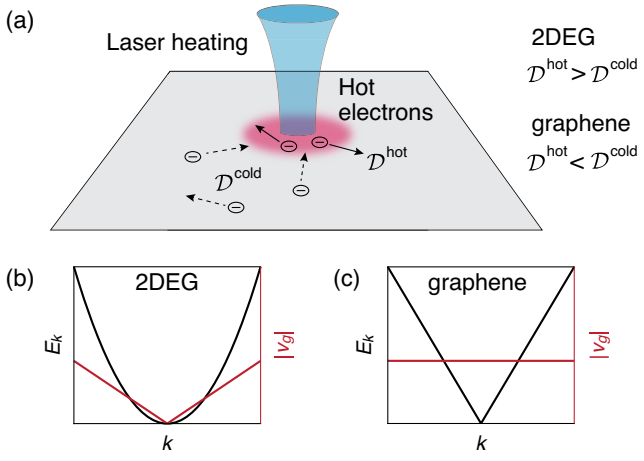


FIG. 1. (a) Illustration of a two dimensional system illuminated by a focused continuous-wave laser beam to locally heat electrons (red region). (b),(c) Energy dispersion and group velocity of (b) free electrons in a 2DEG and (c) MDFs in graphene. The electron diffusion direction is determined by the temperature dependence of the diffusivity coefficient $\mathcal{D} = \langle v^2 \rangle \langle \tau \rangle$, which displays the qualitative behavior summarized in (a) (right text), as derived from the electron group velocity in (b) and (c). Normal and anomalous electron diffusion are predicted in the 2DEG and graphene, respectively.

*Diffusion coefficients and energy-dependent relaxation.*—Although it is not a rigourous procedure, we first estimate the temperature dependence of the electrons using the conventional definition of the diffusion coefficient $\mathcal{D} = \langle v^2 \rangle \langle \tau \rangle$. A more rigorous model is presented in next section. The mean square velocity of 2DEG electrons is determined by the their thermal energy $m_e \langle v^2 \rangle / 2 = \langle E_T \rangle - \langle E_{T=0} \rangle$ at temperature $T$ [22], and for MDFs in graphene one trivially gets $\langle v^2 \rangle = v_F^2$.

Both the definition of $\mathcal{D}$ and the more rigourous model used below require information on the energy dependence of the relaxation time $\tau(E)$. In $\mathcal{D}$, the latter enters through the average $\langle \tau \rangle = \int dE\, N(E) \tau(E) [-\partial_E f(E)] / \int dE\, N(E) [-\partial_E f(E)]$, where the density of states is $N(E) = m_e / \pi \hbar^2$ for the 2DEG and $N(E) = 2|E| / \pi v_F^2 \hbar^2$ for graphene, and $f(E)$ is the Fermi-Dirac distribution, involving a temperature-dependent chemical potential $\mu(T)$ [22]. Throughout this Letter, the electron energy integral runs over $\{0, +\infty\}$ for the 2DEG and $\{-\infty, +\infty\}$ for graphene. The relaxation time in the latter is taken to satisfy $\tau(-E) = \tau(E)$.

In this Letter, we consider energy-dependent relaxation mechanisms associated with three major processes, corresponding to scattering by impurities, acoustic phonons, and optical phonons. Assuming ionic impurities located on the plane of the 2D material and each of them having a charge $e$, the resulting impurity-scattering rate is given by [23,24]

$$\frac{1}{\tau_{\text{im}}(E_k, T)} = \frac{2\pi n_{\text{i}}}{\hbar} \sum_{\ell \mathbf{k}'} \left| \frac{v_q}{\epsilon} \right|^2 F [1 - \cos(\theta_{\mathbf{k}'} - \theta_{\mathbf{k}})] \delta_{k,k'},$$

where $n_i$ is the density of impurities, $\ell$ runs over the two $\pi$ bands in graphene with energies $E_k = \pm v_F \hbar |k|$, $\ell = 1$ for the 2DEG, $v_q = 2\pi e^2 / q$ is the 2D Fourier component of the Coulomb potential with wave vector $\mathbf{q} = \mathbf{k}' - \mathbf{k}$, $F = 1$ for the 2DEG, and $F = [1 + \cos(\theta_{\mathbf{k}'} - \theta_{\mathbf{k}})]/2$ for graphene. The temperature dependence is incorporated in the screening function $\epsilon(q, T) = 1 + v_q \chi(q, T)$, where $\chi(q, T)$ is the susceptibility [22,25–27]. Scattering by this type of impurity is dominant in graphene at low and room temperatures [24].

The scattering rate of electrons by acoustic phonons can be written as [22,28,31]

$$\frac{1}{\tau_{\text{ac}}(E, T_l)} = \alpha \frac{\pi D_{\text{ac}}^2}{4\hbar \rho v_{\text{ac}}^2} k_B T_l N(E),$$

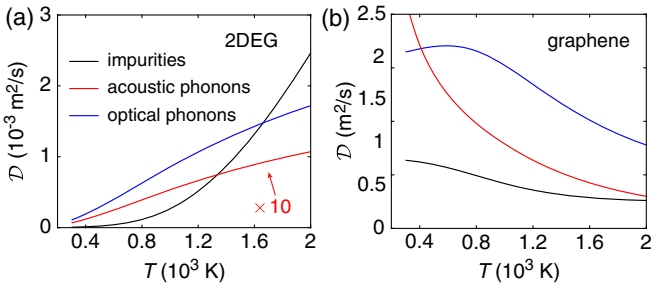


FIG. 2. Electron diffusion coefficient $\mathcal{D}$ in (a) a 2DEG and (b) graphene as a function of temperature. Each curve only considers one scattering mechanism caused by impurities (black), acoustic phonons (blue), or optical phonons (red). The temperature dependence of $\mathcal{D}$ supports the conclusion anticipated in Fig. 1(a). The Fermi level and impurity density are assumed to be $E_F = 0.2$ eV and $n_i = 2 \times 10^{11}$ cm$^{-2}$ in both materials (see main text for other parameters).

and for optical phonons the rate is given by [22,31–33]

$$\frac{1}{\tau_{\rm op}(E,T_l)} = \alpha \frac{\pi D_{\rm op}^2}{8\rho\omega_0} \sum_{\pm} \left[ n_{T_l}(\omega_0) + \frac{1}{2} \pm \frac{1}{2} \right] N(E \mp \hbar\omega_0),$$

where $\alpha = 4$ for the 2DEG and $\alpha = 1$ for graphene, $D_{\rm ac}$ and $D_{\rm op}$ are the deformation potentials of acoustic and optical phonons, $\rho$ is the surface mass density, $\hbar\omega_0$ is the optical phonon energy, and $n_{T_l}(\omega_0)$ is the Bose-Einstein distribution evaluated at the lattice temperature $T_l$. Due to the weak electron-phonon interaction in clean graphene and the 2DEG, $T_l$ can remain close to the ambient level even when the electrons are heated [18], so throughout this Letter we assume $T_l = 300$ K. We also use the effective acoustic velocity $v_{\rm ac}$, defined by $2/v_{\rm ac}^2 = 1/v_{{\rm ac},L}^2 + 1/v_{{\rm ac},T}^2$ and accounting for both longitudinal and transverse phonons [31].

With the energy and temperature dependent $\tau$ obtained from the above equations, we can readily find the diffusion coefficient $\mathcal{D}$ for electrons at different temperatures, as shown in Fig. 2. For both 2DEG and graphene we use the same parameters $D_{\rm ac} = 9.94$ eV, $D_{\rm op} = 5 \times 10^9$ eV/cm, $\hbar\omega_0 = 200$ meV, $\rho = 7.6 \times 10^{-8}$ g/cm$^2$, and $v_{\rm ac} = 1.62 \times 10^6$ cm/s, which are in fact chosen to be consistent with the properties of graphene [28,31,33]. Actually, the results presented below on the thermoelectric field do not strongly depend on these parameters. In Fig. 2, for all three scattering mechanisms considered, $\mathcal{D}$ increases monotonically with temperature in the 2DEG, while it decreases for MDFs in graphene at high temperatures, thus confirming normal and anomalous diffusion regimes in the 2DEG and graphene, respectively.

*Model based on the Boltzmann equation.*—A standard and more rigorous description of electron diffusion is based on Boltzmann's transport equation, which is valid for small

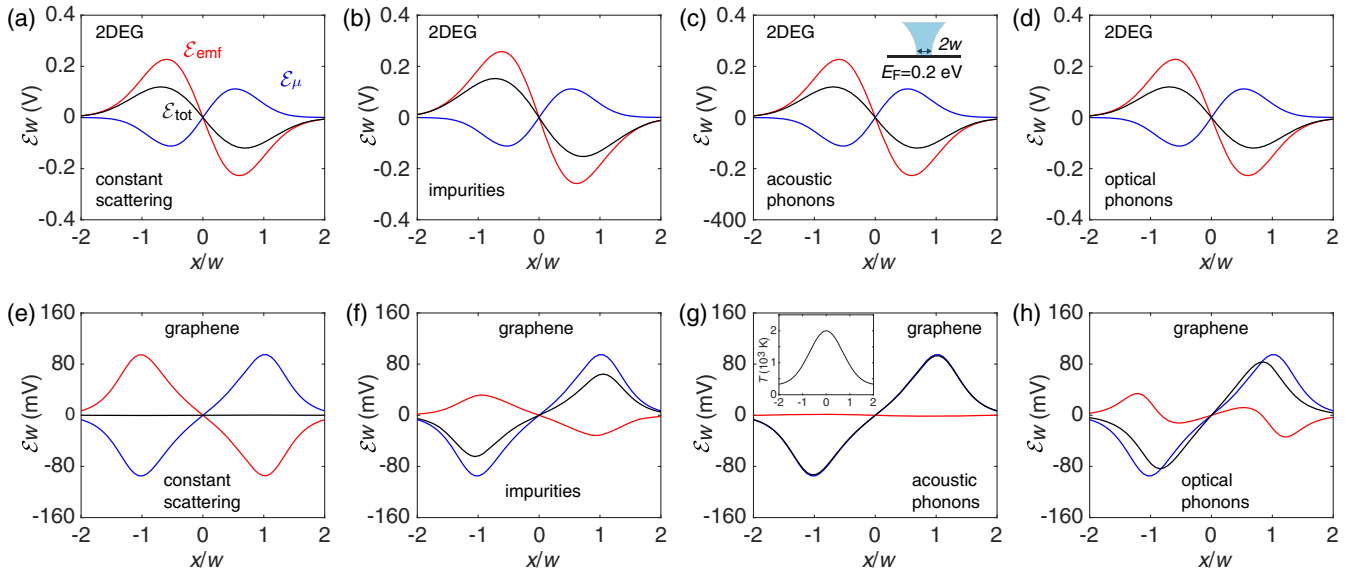


FIG. 3. Thermoelectric field acting on uniform (a)–(d) 2DEG and (e)–(h) graphene films subject to a temperature Gaussian distribution $T(x) = 1700[\mathrm{K}]e^{-x^2/w^2} + 300[\mathrm{K}]$ with $w = 1$ $\mu$m [see insets in (c),(g)]. We consider different models for scattering: (a),(e) a constant scattering rate, (b),(f) impurity scattering, (c),(g) acoustic-phonon scattering, and (d),(h) optical-phonon scattering. Electron diffusion is determined by the total thermoelectric field $\vec{\mathcal{E}}_{\rm tot}$ (black curves), which is the sum of the electromotive field associated with the Seebeck effect $\vec{\mathcal{E}}_{\rm emf}$ (red curves) and an effective field $\vec{\mathcal{E}}_\mu$ (blue curves), arising from the temperature dependence of the chemical potential. The force $-e\vec{\mathcal{E}}_{\rm tot}$ drives electron diffusion opposite and along the temperature gradient in the 2DEG and graphene, respectively, for all scattering mechanisms considered (see signs of $\vec{\mathcal{E}}_{\rm tot}$), except when assuming an unrealistic constant relaxation time in graphene [see (e)], which leads to $\vec{\mathcal{E}}_{\rm tot} = 0$. All parameters are the same as in Fig. 2.

temperature gradients as those considered here. In this model, the total electric field acting on the electrons can be written as [22]

$$\vec{\mathcal{E}}_{\rm tot} = \vec{\mathcal{E}}_{\rm Coul} + \frac{1}{e}\nabla\mu - S\nabla T, \tag{1}$$

where $\vec{\mathcal{E}}_{\rm Coul}$ is the Coulomb electric field produced by the nonuniform electron charge distributions, the second term $\vec{\mathcal{E}}_{\mu} = \nabla\mu/e = (\partial_T\mu)\nabla T/e$ is due to the temperature dependence of the chemical potential, and $\vec{\mathcal{E}}_{\rm emf} = -S\nabla T$ is the electromotive field in the Seebeck effect. In fact, for uncharged particles, we have $\vec{\mathcal{E}}_{\rm Coul} = 0$ and the particle current is then $\propto -\nabla T$, with the prefactor approximately given by the diffusion coefficient $\mathcal{D}$ discussed above. It should be noted that for most studies on thermoelectricity, the field component $\vec{\mathcal{E}}_{\mu}$ is combined with $\vec{\mathcal{E}}_{\rm Coul}$ to define an electrochemical potential that corresponds to the voltage measurable through an external electric circuit (e.g., a thermocouple). However, for closed systems such as in Fig. 1(a), the direction of electron diffusion depends on the details of both $\vec{\mathcal{E}}_{\mu}$ and $\vec{\mathcal{E}}_{\rm emf}$. In particular, the Seebeck coefficient is given by $S = -\mathcal{J}_1/\mathcal{J}_0 eT$ in terms of $\mathcal{J}_m = (\pi\hbar^2)^{-1}\int |E| dE \tau(E)(E-\mu)^m[-\partial_E f(E)]$.

*Thermoelectric field acting on the material electrons.*—In Fig. 3, we show calculations of the thermoelectric field acting on electrons in a 2DEG [Figs. 3(a)–3(d)] and graphene [Figs. 3(e)–3(h)] assuming a uniform density (i.e., $\vec{\mathcal{E}}_{\rm Coul} = 0$). We also assume that heating by a focused laser beam leads to a Gaussian temperature distribution in these 2D systems [see insets in Figs. 3(c) and 3(g)]. To disentangle the contributions of different relaxation mechanisms, we only consider the energy-dependent relaxation time $\tau(\epsilon)$ through a single scattering channel in each plot of Fig. 3. In addition to scattering associated with impurities [Figs. 3(b) and 3(f)] and phonons [Figs. 3(c), 3(d), 3(g), and 3(h)], as investigated in Fig. 2, we also include here results obtained for a constant relaxation time $\tau_{\rm const}$ [Figs. 3(a) and 3(e)]. Noticing that $\vec{\mathcal{E}}_{\mu}$ is a material property, and also that both a constant prefactor in $\tau(E)$ and the chosen $\tau_{\rm const}$ cancel out in the above definition of the Seebeck coefficient $S$, we conclude that the thermoelectric field is independent of the actual magnitude of $\tau$.

Because of the vanishing of $\vec{\mathcal{E}}_{\rm Coul}$ in homogeneous electron distributions, the total field reduces to $\vec{\mathcal{E}}_{\rm tot} = \vec{\mathcal{E}}_{\rm emf} + \vec{\mathcal{E}}_{\mu}$, so the direction of electron diffusion is determined by the relative magnitude of $\vec{\mathcal{E}}_{\rm emf}$ and $\vec{\mathcal{E}}_{\mu}$. In our calculations, we find the electromotive field $\vec{\mathcal{E}}_{\rm emf}$ (red curves, Fig. 3) to be generally directed along the temperature gradient $\nabla T$ (and so the electromotive force $-e\vec{\mathcal{E}}_{\rm emf}$ is directed opposite to it), which is consistent with the typical negative Seebeck coefficient in electron-doped systems. In contrast, $-e\vec{\mathcal{E}}_{\mu}$ is always along $\nabla T$ because an increase in electron temperature lowers the chemical potential $\mu$ [see Eq. (1) and Ref. [22]].

For a 2DEG, all scattering mechanisms similarly result in a thermoelectric field $\vec{\mathcal{E}}_{\rm tot}$ [black curves, Figs. 3(a)–3(d)] directed along $\nabla T$ (i.e., a force $-e\vec{\mathcal{E}}_{\rm tot}$ against $\nabla T$), which confirms that free electrons undergo conventional diffusion. In contrast, for a graphene layer with characteristic scattering processes dominated by impurities and phonons [Figs. 3(f)–3(h)], $\vec{\mathcal{E}}_{\mu}$ exceeds $\vec{\mathcal{E}}_{\rm emf}$, thus resulting in a total force $-e\vec{\mathcal{E}}_{\rm tot}$ directed along $\nabla T$, and therefore producing anomalous diffusion of MDFs. Interestingly, although a constant relaxation time [Fig. 3(b)] can give rise to a nonzero Seebeck effect, $\vec{\mathcal{E}}_{\rm emf}$ is perfectly cancelled by $\vec{\mathcal{E}}_{\mu}$, which confirms our intuitive explanation presented in Fig. 1.

*Charge rearrangement in a temperature gradient.*—The thermoelectric fields $\vec{\mathcal{E}}_{\rm emf}$ and $\vec{\mathcal{E}}_{\mu}$ presented for uniform electrons in Fig. 3 cause further electron diffusion until a steady electron density distribution is established, when $\vec{\mathcal{E}}_{\rm emf} + \vec{\mathcal{E}}_{\mu}$ is balanced by the additional field $\vec{\mathcal{E}}_{\rm Coul}$ produced by the nonuniform charge distribution. The resulting electron rearrangements in the 2DEG and graphene

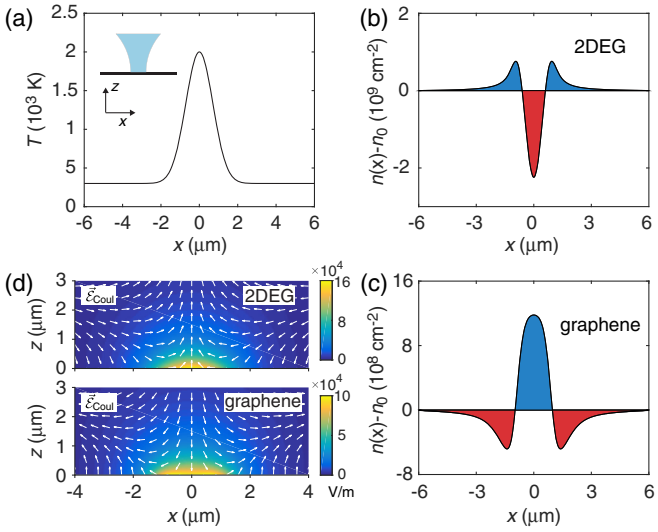


FIG. 4. (a) Illustration of a Gaussian temperature distribution in a 2D system: $T(x) = 1700[\mathrm{K}]e^{-x^2/w^2} + 300[\mathrm{K}]$ with $w = 1$ $\mu$m, produced by focused laser heating (inset). (b),(c) Steady-state electron density in (b) a 2DEG and (c) graphene under the temperature distribution in (a). Here, $n_0$ is the unperturbed electron density, determined by the Fermi level $E_F = 0.2$ eV. (d) Amplitude (color scale) and orientation (arrows) distributions of the static electric fields $\vec{\mathcal{E}}_{\rm Coul}$ generated by the thermally excited nonuniform electron charges [color in (b),(c)]. The 2DEG and graphene are located at $z = 0$. The three scattering mechanisms by impurities and phonons shown in Fig. 3 are all included (i.e., $\tau^{-1} = \tau_{\rm im}^{-1} + \tau_{\rm ac}^{-1} + \tau_{\rm op}^{-1}$) using the same calculation parameters.

systems are shown in Fig. 4. The thermoelectric fields $\vec{\mathcal{E}}_{\mathrm{emf}}$ and the contribution $\vec{\mathcal{E}}_{\mu}$ induced by the temperature gradient can be directly calculated following a similar approach as used to obtain Fig. 3, safely assuming a uniform $E_F$ because the density rearrangement is relatively small. The electric field induced by the nonuniform charge satisfies the Poisson equation $\nabla \cdot \vec{\mathcal{E}}_{\mathrm{Coul}} = -4\pi e n(\mathbf{r})$, which, together with the equilibrium condition $\vec{\mathcal{E}}_{\mathrm{Coul}} = -\vec{\mathcal{E}}_{\mathrm{emf}} - \vec{\mathcal{E}}_{\mu}$, allows us to easily find the steady charge distributions in the 2DEG [Fig. 4(b)] and graphene [Fig. 4(c)]. The highest temperature gradient around the waist of the Gaussian distribution results in strong outward and inward electron drifts in the normal and anomalous diffusion regimes found in the 2DEG and graphene, respectively. Such electron drifts further decrease or increase the electron density in the temperature Gaussian peak (around $x = 0$) by accumulating or depleting electrons outside the waist. Additionally, nonuniform charge distributions [colors in Figs. 4(b) and 4(c)] associated with the electron density rearrangements can induce a static electric field $\vec{\mathcal{E}}_{\mathrm{Coul}}$ [Fig. 4(d)] to balance the thermoelectric field. For both the 2DEG and graphene, $\vec{\mathcal{E}}_{\mathrm{Coul}}$ is localized around the span of the temperature Gaussian distribution, with its field lines flowing from positive to negative charges accumulated by electron thermodiffusion [see Figs. 4(b) and 4(c)].

*Concluding remarks.*—We expect anomalous thermodiffusion to be observed in the evolution of MDFs supported by various 2D or higher-dimensional materials, such as surface states of topological insulators [34–38] or Dirac semi-metals [39,40]. The concepts of conventional and anomalous thermodiffusion can be straightforwardly generalized to holes in $n$-doped semiconductors and graphene. In addition, the Seebeck coefficients of electrons in some metals (e.g., nickel and potassium) are intrinsically positive. We expect that anomalous electron thermodiffusion will also be found in such materials. Considering a one-dimensional tight-binding electron band $E_k = E_0 - 2t \times \cos(ka)$, the group velocity decreases with electron energy in the $E_k > E_0$ regime, so anomalous thermodiffusion can also be anticipated in this simple model for a Fermi level $E_F > E_0$ according to the condition illustrated in Fig. 1.

Our findings are important for a fundamental understandings of the evolution of electrons in a material subject to a temperature gradient, which can be relevant to applications in thermopower generation. The processes of electron thermodiffusion here revealed can be related to branches of physics dealing with electron systems in nonuniform temperature environments. For example, when further considering the dynamical establishment of a nonuniform charge density as shown in Figs. 4(b) and 4(c), a focused laser pulse can directly excite charge oscillations in extended graphene [22], thus offering a sought-after way to generate graphene plasmons in extended homogeneous layers without resorting to scattering structures [41–43], such as the tips commonly used in scanning near-field optical microscopy [29,44,45]. The interaction between the electric field induced by thermally excited charges and neighboring molecules could lead to a new way of performing nonlinear optical sensing [46–48]. The electric potential built up by a nonuniform electron charge distribution as shown in Fig. 4(d) could interact with an electron beam and thus provide a potential alternative to realize a phase plate for ultrafast electron beam shaping [49–51].

This work has been supported in part by NSFC (Grant No. 12004117), ERC (Advanced Grant No. 789104-eNANO), the Spanish MINECO (Grants No. MAT2017-88492-R and No. SEV2015-0522), the Catalan CERCA Program, and Fundacio Privada Cellex

*Deng.Pan@icfo.eu
†javier.garciadeabajo@nanophotonics.es

[1] S. Duhr and D. Braun, Proc. Natl. Acad. Sci. U.S.A. **103**, 19678 (2006).
[2] M. Reichl, M. Herzog, A. Götz, and D. Braun, Phys. Rev. Lett. **112**, 198101 (2014).
[3] C. J. Wienken, P. Baaske, U. Rothbauer, D. Braun, and S. Duhr, Nat. Commun. **1**, 100 (2010).
[4] P. A. Schoen, J. H. Walther, S. Arcidiacono, D. Poulikakos, and P. Koumoutsakos, Nano Lett. **6**, 1910 (2006).
[5] A. Barreiro, R. Rurali, E. R. Hernández, J. Moser, T. Pichler, L. Forro, and A. Bachtold, Science **320**, 775 (2008).
[6] H.-R. Jiang, H. Wada, N. Yoshinaga, and M. Sano, Phys. Rev. Lett. **102**, 208301 (2009).
[7] J. Daniels, Z. Phys. **203**, 235 (1967).
[8] P. Blanco, M. M. Bou-Ali, J. K. Platten, D. A. de Mezquia, J. A. Madariaga, and C. Santamaría, J. Chem. Phys. **132**, 114506 (2010).
[9] E. Bringuier and A. Bourdon, Physica (Amsterdam) **385A**, 9 (2007).
[10] B.-J. de Gans, R. Kita, B. Müller, and S. Wiegand, J. Chem. Phys. **118**, 8073 (2003).
[11] H. Haug and S. W. Koch, *Quantum Theory of the Optical and Electronic Properties of Semiconductors* (World Scientific, Singapore, 2009).
[12] K. S. Novoselov, A. K. Geim, S. V. Morozov, D. Jiang, Y. Zhang, S. V. Dubonos, I. V. Grigorieva, and A. A. Firsov, Science **306**, 666 (2004).
[13] A. H. Castro Neto, F. Guinea, N. M. R. Peres, K. S. Novoselov, and A. K. Geim, Rev. Mod. Phys. **81**, 109 (2009).
[14] Y. M. Zuev, W. Chang, and P. Kim, Phys. Rev. Lett. **102**, 096807 (2009).
[15] P. Wei, W. Bao, Y. Pu, C. N. Lau, and J. Shi, Phys. Rev. Lett. **102**, 166808 (2009).
[16] V. Shautsova, T. Sidiropoulos, X. Xiao, N. A. Güsken, N. C. Black, A. M. Gilbertson, V. Giannini, S. A. Maier, L. F. Cohen, and R. F. Oulton, Nat. Commun. **9**, 5190 (2018).

[17] D. Brida, A. Tomadin, C. Manzoni, Y. J. Kim, A. Lombardo, S. Milana, R. R. Nair, K. S. Novoselov, A. C. Ferrari, G. Cerullo *et al.*, Nat. Commun. **4**, 1987 (2013).
[18] I. Gierz, J. C. Petersen, M. Mitrano, C. Cacho, I. C. E. Turcu, E. Springate, A. Stöhr, A. Köhler, U. Starke, and A. Cavalleri, Nat. Mater. **12**, 1119 (2013).
[19] M. Wagner, Z. Fei, A. S. McLeod, A. S. Rodin, W. Bao, E. G. Iwinski, Z. Zhao, M. Goldflam, M. Liu, G. Dominguez *et al.*, Nano Lett. **14**, 894 (2014).
[20] G. X. Ni, L. Wang, M. D. Goldflam, M. Wagner, Z. Fei, A. S. McLeod, M. K. Liu, F. Keilmann, B. Özyilmaz, A. H. C. Neto *et al.*, Nat. Photonics **10**, 244 (2016).
[21] A. Tomadin, S. M. Hornett, H. I. Wang, E. M. Alexeev, A. Candini, C. Coletti, D. Turchinovich, M. Kläui, M. Bonn, F. H. Koppens *et al.*, Sci. Adv. **4**, eaar5313 (2018).
[22] See the Supplemental Material at http://link.aps.org/supplemental/10.1103/PhysRevLett.125.176802 for details on the temperature-dependent quantities of 2DEG and graphene (including the chemical potential and the electron thermal energy), simple derivations of the scattering rates by impurites and phonons, and preliminary results on the plasmon generation by pulsed laser heating, which includes Refs. [11,23–30].
[23] T. Ando, J. Phys. Soc. Jpn. **75**, 074716 (2006).
[24] E. H. Hwang, S. Adam, and S. Das Sarma, Phys. Rev. Lett. **98**, 186806 (2007).
[25] T. Ando, A. B. Fowler, and F. Stern, Rev. Mod. Phys. **54**, 437 (1982).
[26] B. Wunsch, T. Stauber, F. Sols, and F. Guinea, New J. Phys. **8**, 318 (2006).
[27] E. H. Hwang and S. Das Sarma, Phys. Rev. B **75**, 205418 (2007).
[28] E. H. Hwang and S. Das Sarma, Phys. Rev. B **77**, 115449 (2008).
[29] M. B. Lundeberg, Y. Gao, R. Asgari, C. Tan, B. V. Duppen, M. Autore, P. Alonso-González, A. Woessner, K. Watanabe, T. Taniguchi *et al.*, Science **357**, 187 (2017).
[30] P. F. Maldague, Surf. Sci. **73**, 296 (1978).
[31] T. Sohier, M. Calandra, C.-H. Park, N. Bonini, N. Marzari, and F. Mauri, Phys. Rev. B **90**, 125414 (2014).
[32] N. Sule and I. Knezevic, J. Appl. Phys. **112**, 053702 (2012).
[33] H. A. Hafez, I. Al-Naib, M. M. Dignam, Y. Sekine, K. Oguri, F. Blanchard, D. G. Cooke, S. Tanaka, F. Komori, H. Hibino *et al.*, Phys. Rev. B **91**, 035422 (2015).
[34] C. L. Kane and E. J. Mele, Phys. Rev. Lett. **95**, 146802 (2005).
[35] M. König, S. Wiedmann, C. Brüne, A. Roth, H. Buhmann, L. W. Molenkamp, X.-L. Qi, and S.-C. Zhang, Science **318**, 766 (2007).
[36] L. Fu and C. L. Kane, Phys. Rev. B **76**, 045302 (2007).
[37] D. Hsieh, D. Qian, L. Wray, Y. Xia, Y. S. Hor, R. J. Cava, and M. Z. Hasan, Nature (London) **452**, 970 (2008).
[38] P. Di Pietro, M. Ortolani, O. Limaj, A. Di Gaspare, V. Giliberti, F. Giorgianni, M. Brahlek, N. Bansal, N. Koirala, S. Oh *et al.*, Nat. Nanotechnol. **8**, 556 (2013).
[39] S. M. Young, S. Zaheer, J. C. Y. Teo, C. L. Kane, E. J. Mele, and A. M. Rappe, Phys. Rev. Lett. **108**, 140405 (2012).
[40] Z. Liu, B. Zhou, Y. Zhang, Z. Wang, H. Weng, D. Prabhakaran, S.-K. Mo, Z. Shen, Z. Fang, X. Dai *et al.*, Science **343**, 864 (2014).
[41] T. J. Constant, S. M. Hornett, D. E. Chang, and E. Hendry, Nat. Phys. **12**, 124 (2016).
[42] T. A. Morgado and M. G. Silveirinha, Phys. Rev. Lett. **119**, 133901 (2017).
[43] R. Yu, Q. Guo, F. Xia, and F. J. García de Abajo, Phys. Rev. Lett. **121**, 057404 (2018).
[44] J. Chen, M. Badioli, P. Alonso-González, S. Thongrattanasiri, F. Huth, J. Osmond, M. Spasenović, A. Centeno, A. Pesquera, P. Godignon *et al.*, Nature (London) **487**, 77 (2012).
[45] Z. Fei, A. S. Rodin, G. O. Andreev, W. Bao, A. S. McLeod, M. Wagner, L. M. Zhang, Z. Zhao, M. Thiemens, G. Dominguez *et al.*, Nature (London) **487**, 82 (2012).
[46] D. Rodrigo, O. Limaj, D. Janner, D. Etezadi, F. J. García de Abajo, V. Pruneri, and H. Altug, Science **349**, 165 (2015).
[47] R. Yu, J. D. Cox, and F. J. García de Abajo, Phys. Rev. Lett. **117**, 123904 (2016).
[48] Q. Guo, R. Yu, C. Li, S. Yuan, B. Deng, F. J. García de Abajo, and F. Xia, Nat. Mater. **17**, 986 (2018).
[49] W. Cai, O. Reinhardt, I. Kaminer, and F. J. García de Abajo, Phys. Rev. B **98**, 045424 (2018).
[50] G. M. Vanacore, G. Berruto, I. Madan, E. Pomarico, P. Biagioni, R. J. Lamb, D. McGrouther, O. Reinhardt, I. Kaminer, B. Barwick *et al.*, Nat. Mater. **18**, 573 (2019).
[51] A. Konečná and F. J. García de Abajo, Phys. Rev. Lett. **125**, 030801 (2020).